Supplementary Material

Role of Br-Cl distribution uniformity on the spectral stability of blue emitting mixed-halide perovskites

Dan Chen, Yu Mao, Xianglan Huang, Jichen Zhao, Zhiyuan Zhang, Jian Wang* and Junbiao Peng

Institute of Polymer Optoelectronic Materials and Devices, State Key Laboratory of Luminescent Materials and Devices, South China University of Technology, Guangzhou 510640, China. E-mail: jianwang@scut.edu.cn

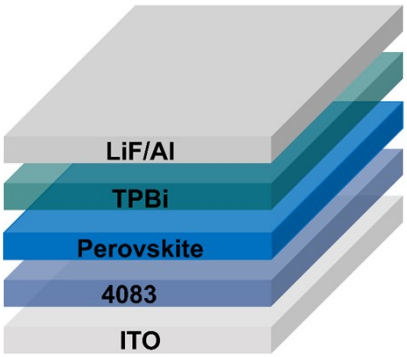

Figure S1. Schematic illustration of the device configuration.

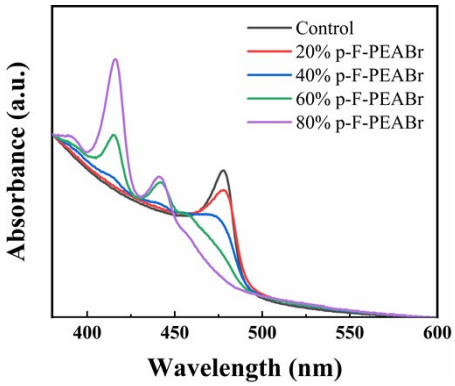

Figure S2. UV-vis absorption spectrum of $CsPbClBr_2$ doped with different concentrations of p-F-PEABr.

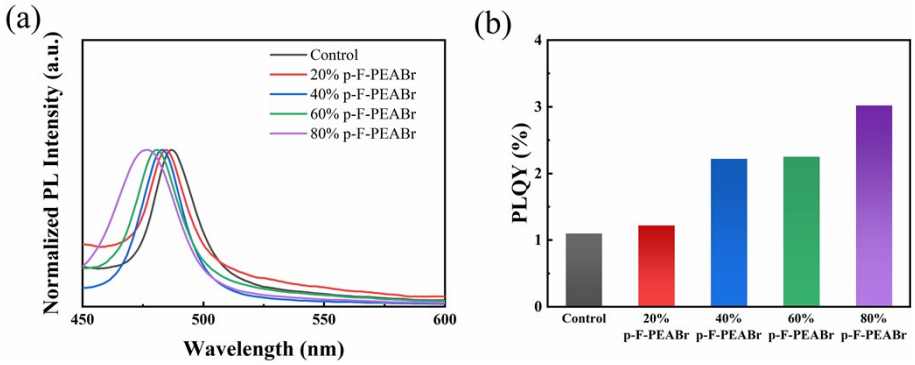

Figure S3. (a) PL spectra, and (b) PLQY of $CsPbClBr_2$ doped with different concentrations of p-F-PEABr.

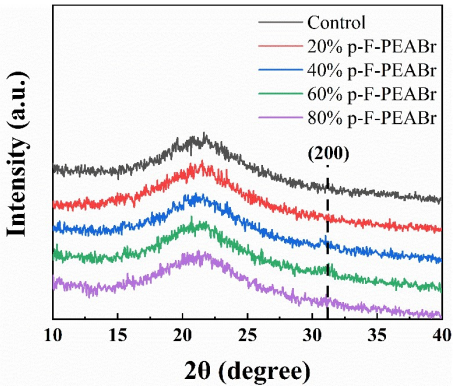

Figure S4. XRD patterns of $CsPbClBr_2$ doped with different concentrations of p-F-PEABr.

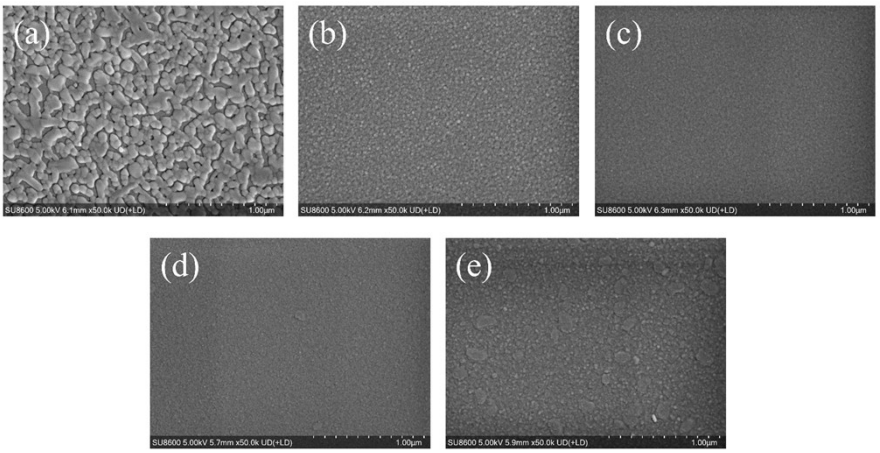

Figure S5. SEM images of $CsPbClBr_2$ doped with different concentrations of p-F-PEABr: (a) Control, (b) 20 %, (c) 40 %, (d) 60 %, (e) 80 %.

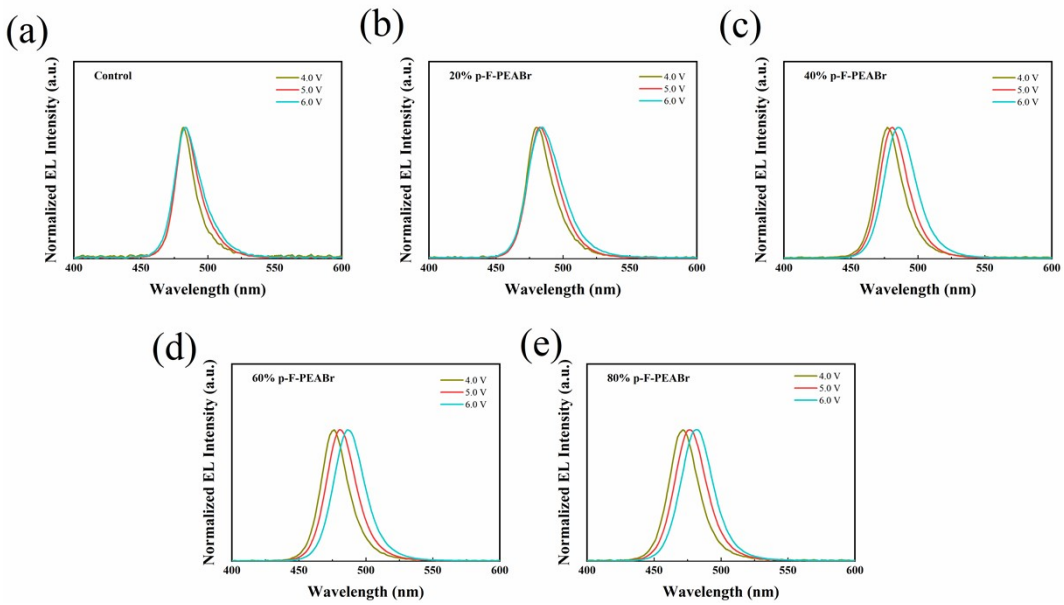

Figure S6. The EL spectrum of the representative PeLEDs: (a) Control, (b) 20% p-F-PEABr, (c) 40% p-F-PEABr, (d) 60% p-F-PEABr, (e) 80% p-F-PEABr.

Table S1. EL peak shift of $CsPbClBr_2$ doped with different concentrations of p-F-PEABr.

p-F-PEABr (%)	EL peak at 4V (nm)	EL peak at 6V (nm)	Red shift of EL peak (nm)
0	481.8	483.3	1.5
20	480.3	484.3	4.0
40	477.1	485.0	7.9
60	476.3	486.6	10.3
80	471.6	481.9	10.3

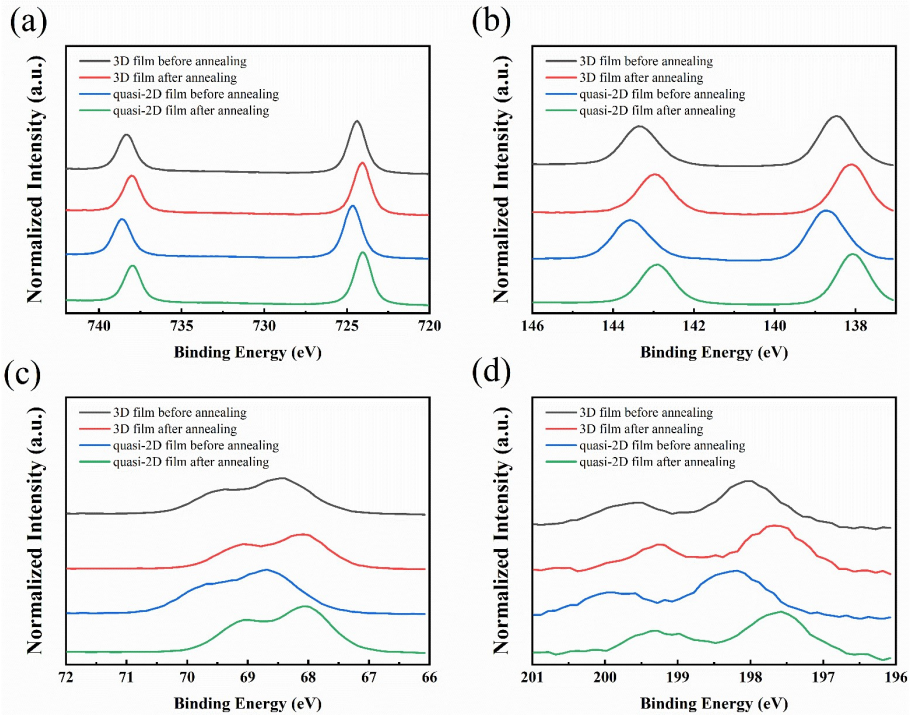

Figure S7. XPS spectra of 3D and quasi-2D films before and after annealing: (a) Cs 3d, (b) Pb 4f, (c) Br 3d, (d) Cl 2p.

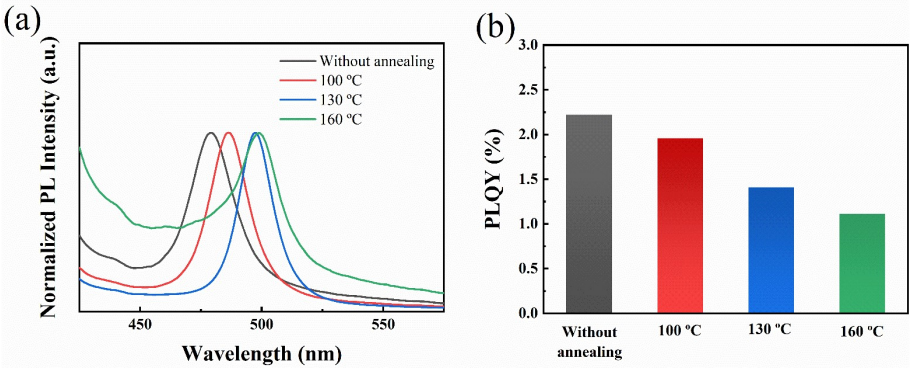

Figure S8. (a) PL spectra, and (b) PLQY of 40% p-F-PEABr doped $CsPbClBr_2$ film after annealing at different annealing temperatures.

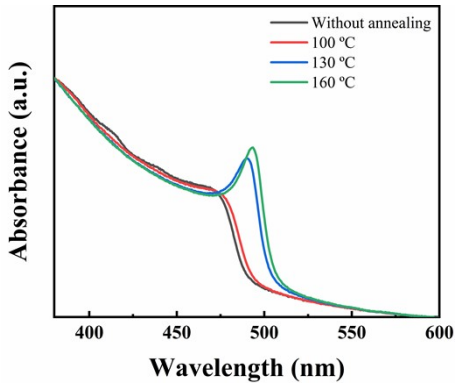

Figure S9. UV-vis spectra of 40% p-F-PEABr doped $CsPbClBr_2$ film after annealing at different annealing temperatures.

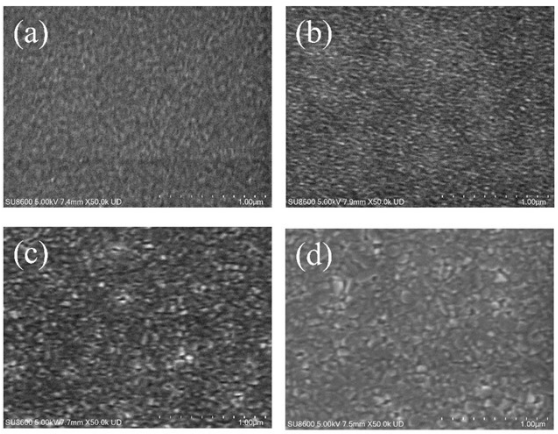

Figure S10. SEM images of 40% p-F-PEABr doped $CsPbClBr_2$ film after annealing at different annealing temperatures: (a) without annealing, (b) 100 ºC, (c) 130 ºC, (d) 160 ºC.

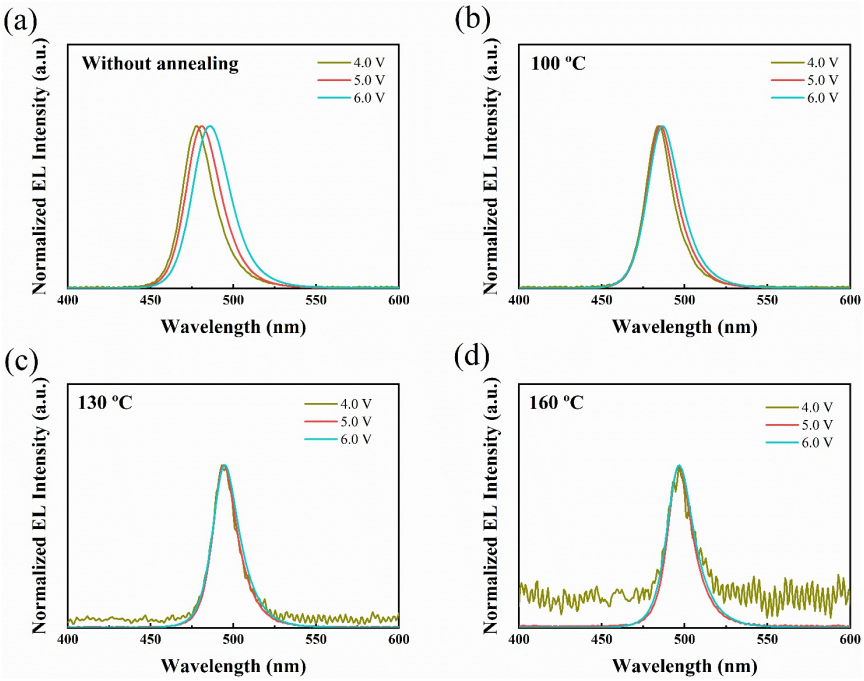

Figure S11. The EL spectrum of the representative PeLEDs at different annealing temperatures: (a) without annealing, (b) 100 ºC, (c) 130 ºC, (d) 160 ºC.

Table S2. EL peak shifts of 40% p-F-PEABr doped $CsPbClBr_2$ PeLEDs at different annealing temperatures.

Annealing temperatures (ºC)	EL peak at 4 V (nm)	EL peak at 6 V (nm)	Red shift of EL peak (nm)
Without annealing	477.1	485.0	7.9
100	484.3	486.9	2.6
130	493.0	494.0	1.0
160	496.1	496.3	0.2

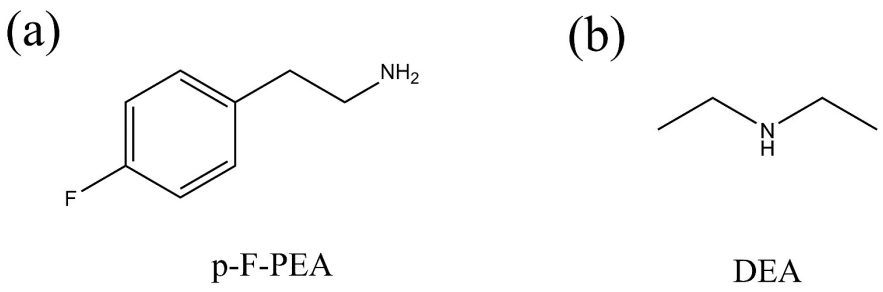

Figure S12. Molecular structures of p-F-PEA and DEA.

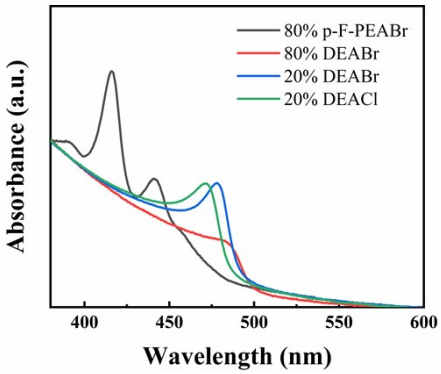

Figure S13. UV-vis spectra of $CsPbClBr_2$ films doped by different dopants.

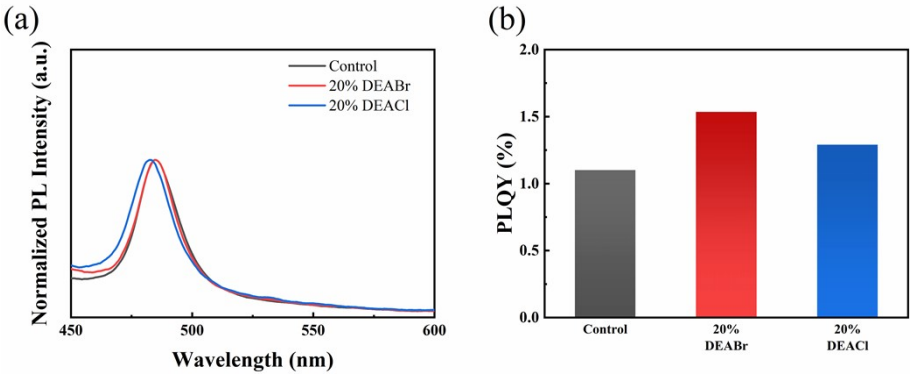

Figure S14. (a) PL spectra, and (b) PLQY of 20% DEABr, and 20% DEACl doped $CsPbClBr_2$ films.

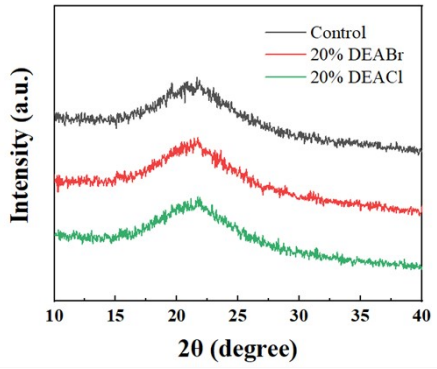

Figure S15. XRD patterns of 20% DEABr, and 20% DEACl doped $CsPbClBr_2$ films.

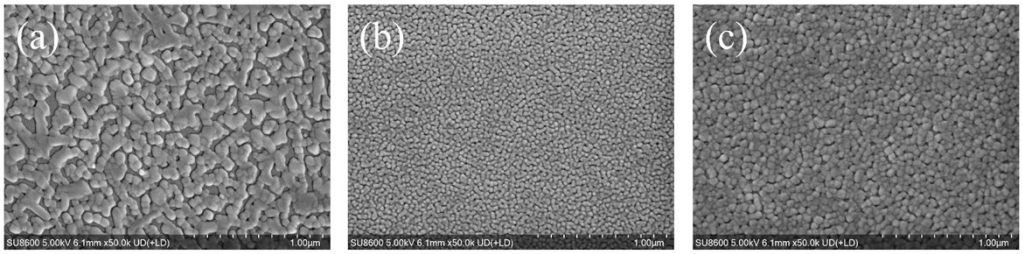

Figure S16. SEM images of 20% DEABr, and 20% DEACl doped $CsPbClBr_2$ films: (a) Control, (b) 20% DEABr, (c) 20% DEACl.

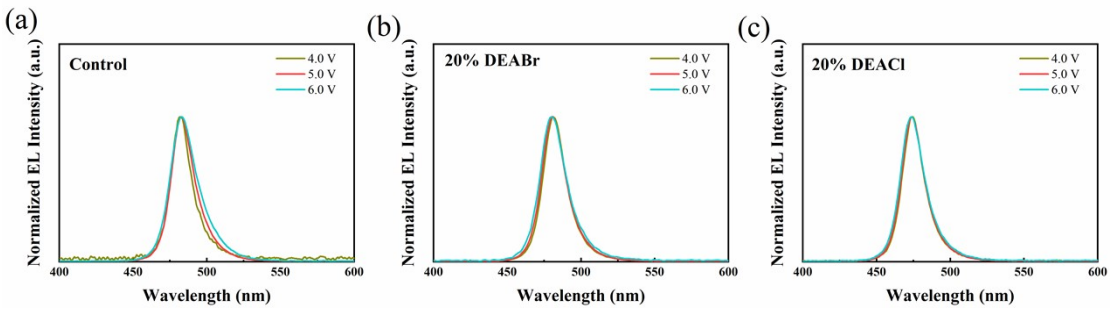

Figure S17. The EL spectra of the representative PeLEDs: (a) Control, (b) 20% DEABr, (c) 20% DEACl.

Table S3. EL peak shifts of 20% DEABr, and 20% DEACl doped $CsPbClBr_2$ PeLEDs.

Emitter	EL peak at 4V (nm)	EL peak at 6V (nm)	Red shift of EL peak (nm)
Control	481.8	483.3	1.5
20% DEABr	481.9	482.2	0.3
20% DEACl	474.0	473.6	-0.4